


## Article

# Buffeting Response Prediction of Long-Span Bridges Based on Different Wind Tunnel Test Techniques

Yi Su <sup>1,2</sup> , Jin Di <sup>1,2,\*</sup>, Shaopeng Li <sup>1,2,\*</sup>, Bin Jian <sup>3</sup> and Jun Liu <sup>4</sup>

<sup>1</sup> Key Laboratory of New Technology for Construction of Cities in Mountain Area, Chongqing University, Chongqing 400450, China; windsu888@cqu.edu.cn

<sup>2</sup> College of Civil Engineering, Chongqing University, Chongqing 400450, China

<sup>3</sup> Research Centre for Wind Engineering, Southwest Jiaotong University, Chengdu 610031, China; janebim@126.com

<sup>4</sup> School of Civil Engineering and Geomatics, Southwest Petroleum University, Chengdu 610500, China; liujun\_sichuan@126.com

\* Correspondence: dijin@cqu.edu.cn (J.D.); lishaopeng0314@163.com (S.L.)

**Abstract:** The traditional method for calculating the buffeting response of long-span bridges follows the strip assumption, and is carried out by identifying aerodynamic parameters through sectional model force or pressure measurement wind tunnel tests. However, there has been no report on predicting the buffeting response based on the sectional model vibration test. In recent years, the author has proposed a method, based on the integrated transfer function, for predicting the buffeting response of long-span bridges through theoretical and full-bridge tests. This provided an idea for predicting the buffeting response based on the sectional model vibration test. Unfortunately, the effectiveness and accuracy of this method have not been proven or demonstrated through effective tests. To solve this problem, a long-span suspension bridge was taken as a background. Parameters such as aerodynamic admittance were identified through a sectional model force measurement test and the integrated transfer functions were identified through a sectional model vibration test. A taut strip model test was also conducted. Furthermore, the buffeting response prediction results based on three kinds of wind tunnel test techniques were compared. The results showed that if the strip assumption was established, the results of the three methods aligned well, and that selecting a reasonable model aspect ratio for the test could effectively reduce the influence of the 3D effect; moreover, identifying the integrated transfer function by the sectional model vibration test could effectively predict the long-span bridge buffeting response. Furthermore, when the strip assumption failed, the results of the traditional calculation method using 3D aerodynamic admittance became smaller. A larger result would be obtained by neglecting the influence of aerodynamic admittance.

**Keywords:** long-span bridge; buffeting response; wind tunnel test; sectional model; aerodynamic admittance; integrated transfer function



**Citation:** Su, Y.; Di, J.; Li, S.; Jian, B.; Liu, J. Buffeting Response Prediction of Long-Span Bridges Based on Different Wind Tunnel Test Techniques. *Appl. Sci.* **2022**, *12*, 3171. <https://doi.org/10.3390/app12063171>

Academic Editors: Wenli Chen, Zifeng Yang, Gang Hu, Haiquan Jing and Junlei Wang

Received: 21 February 2022

Accepted: 16 March 2022

Published: 20 March 2022

**Publisher's Note:** MDPI stays neutral with regard to jurisdictional claims in published maps and institutional affiliations.



**Copyright:** © 2022 by the authors. Licensee MDPI, Basel, Switzerland. This article is an open access article distributed under the terms and conditions of the Creative Commons Attribution (CC BY) license (<https://creativecommons.org/licenses/by/4.0/>).

## 1. Introduction

Among the many vibration forms of bridge structures, buffeting is a random forced vibration generated by the structure under the action of natural wind fluctuation components. It is one of the main areas of research content for the wind-induced vibration of long-span bridges. Low wind speed causes buffeting, and continuous buffeting may cause local fatigue failure of the bridge structure, affecting the bridge's lifespan. In addition, excessive buffeting response of a bridge structure under strong winds negatively affects the safety of construction personnel, equipment, and the comfort of drivers and pedestrians during the operation of the structure. Its concept was proposed in 1930 and originated from the vibration of aircraft in turbulent flow [1]. In the mid-1950s, Scruton first used the concept of buffeting to describe the forced vibration caused by wake flow when he was studying the dynamic response of the Runcorn–Widnes bridge [2]. The theoretical analysis

of the buffeting problem of long-span bridges began when Davenport [3,4] applied the statistical analysis method of buffeting in the aviation field to bridge structures. In the 1960s, based on the theory of aerodynamics, Davenport [3,4] took the lead in proposing the concept of aerodynamic admittance, defined the joint acceptance function, and considered the time and space distribution of the aerodynamic force on the structure. Furthermore, the spanwise correlation of the fluctuating wind was used to describe the spanwise correlation of the buffeting force, and a relatively complete buffeting analysis method for long-span bridges and other slender linear structures was established. In the 1970s, Scanlan et al. [5–8] extended their research results from the flutter theory to the analysis of the buffeting response, and believed that the self-excited force in the flutter analysis would affect the buffeting response of the bridge structure. They expressed the self-excited force caused by structural motion in the form of flutter derivatives, used aerodynamic stiffness and aerodynamic damping to modify Davenport's theory, and then introduced the mechanical admittance function to reflect the influence of structural motion on the system transfer function. Since then, Davenport's buffeting theory, in combination with Scanlan's theory, has become the basis for the theoretical buffeting analysis and calculation method for long-span bridge structures. In the following decades, many scholars [9–15] did fruitful work regarding the buffeting response prediction for long-span bridges under turbulent flow.

So far, the buffeting response has mainly been obtained by two methods: wind tunnel tests and theoretical calculation. The latter is usually based on the principle of aerodynamics, establishes a mathematical model of the relevant wind load, and then applies the structural dynamics method to solve the wind-induced response of the structure. The current theoretical method is based on the pioneering work achieved by Davenport, Scanlan, etc., and has been improved in many subsequent studies. However, due to the characteristics of atmospheric turbulence and the complexity and diversity of bridge section forms, a perfect analytical model cannot be established for the prediction of the buffeting response of bridges. It is difficult to calculate the aerodynamic force and wind-induced responses of bridge structures through purely theoretical analysis. The wind tunnel test is an indispensable and important method, and is still mainly used to identify parameters such as aerodynamic admittance and flutter derivatives.

At present, wind tunnel test techniques [16–18] for long-span bridge buffeting response prediction are divided into three categories: full-bridge aeroelastic model wind tunnel tests, taut strip model wind tunnel tests and sectional model wind tunnel tests. Among them, the full-bridge aeroelastic model wind tunnel test is the most direct test method for measuring the buffeting response of long-span bridges. Based on accurately simulating the bridge model, it directly measures the dynamic response of the bridge to the wind in a simulated natural wind field, and then converts the response of the model measured in the test to the real bridge through a scale ratio. This method is a complete-scale simulation of a real bridge, which can naturally simulate the bridge's three-dimensional aeroelastic effect and dynamic mode shape. It obtains the buffeting response of the bridge more intuitively, and avoids the identification of the aerodynamic parameters of the bridge section. However, the full-bridge test features the drawbacks of high cost, lengthy duration, and difficult model design and production. With the continuous increase of current bridge spans, full-bridge tests of long-span bridges require larger test wind tunnel sizes. In contrast, the sectional model mainly simulates the mid-span section of the main span of the bridge according to the geometric similarity principle, and has a large scale ratio. It has the advantages of low cost, less difficulty in design and production, short preparation time, etc. In addition, the shape of the sectional model can easily be changed, and the aerodynamic shape of the bridge can be optimized in time according to the test results, so it is more widely used. For the prediction of the buffeting response of long-span bridges, the sectional model test is an important auxiliary means of conducting the theoretical calculation method. The theoretical calculation of the buffeting response of long-span bridges has always used sectional model tests to identify the unsteady aerodynamic parameters of the bridge sections. The buffeting response of the bridge is then obtained through the buffeting analysis theory. However,

because the sectional model wind tunnel test cannot simulate turbulent flow fields with large turbulence integral scales, the three-dimensional effect has affected the prediction results of the buffeting response for many years. In recent years, many scholars have proposed empirical correction methods for this problem, but they have not solved the problem with respect to the theoretical foundation or experimental technology [19]. The taut strip model, an aeroelastic model between the full-bridge aeroelastic model and the sectional model, has often been used in previous studies to compare and analyze the difference between the test results of the sectional model and the full-bridge aeroelastic model. The taut strip model test is used to measure the buffeting response of the bridge girder under the condition that the additional aerodynamic interference caused by the structural auxiliary facilities (such as suspenders, cables, towers, etc.) is eliminated. The method considers the first several vibration modes of the bridge, and can consider both the two-dimensional effect of the sectional model and the three-dimensional vibration effect of the bridge structure.

For a long time, sectional model tests only used force and pressure measurements to identify the aerodynamic admittance to assist with the theoretical calculations [20]. Due to the influence of factors such as the applicability of the strip assumption [21,22], there is no case wherein the buffeting response of long-span bridges is predicted by sectional model vibration tests. However, the force measurement test is difficult in the early leveling, correlation measurement, etc., and the accuracy is difficult to guarantee; the pressure measurement test has limitations such as the inability to measure the truss girder and accurately measure the overall force of the bridge in the completed state. In addition, Yan et al. [23] identified the aerodynamic admittance of the bridge section in the free vibration state. The results show that the aerodynamic admittance is related to the vibration state of the main girder, so it is necessary to consider the effect of the actual bridge vibration on the aerodynamic admittance [24,25]. This makes the prediction results biased by the traditional calculation method based on the rigid sectional model pressure or force measurement test to identify aerodynamic admittance on account of the ignorance of the vibration of the structure. Fortunately, the vibration test can effectively avoid the limitations of force and pressure tests. At the same time, it can truly reflect the structural motion state, and comprehensively consider the effects of self-excited force terms such as aerodynamic damping and aerodynamic stiffness. Recently, Su et al. [26] proposed the concept of the integrated transfer function based on the research of Li et al. [27–29] on the influence of the structural aspect ratio on the three-dimensional effect of turbulence, and gave a long-span bridge buffeting response prediction method based on the integrated transfer function. The method points out that the aspect ratio of the test model will have a significant impact on the prediction accuracy of the buffeting response, and can correct the deviation of the prediction result of the buffeting response caused by the inaccurate simulation of the wind field parameters in the wind tunnel. However, even though Su et al. [26] proved the feasibility of the integrated transfer function in the prediction of the buffeting response of long-span bridges through rigorous theoretical derivation and verified the independence of the integrated transfer function from the wind field characteristics through full-bridge aeroelastic model wind tunnel tests, they only expected the results to provide ideas for the buffeting response prediction of long-span bridges based on the identification of integrated transfer functions, and the accuracy and effectiveness of the method have not been directly verified by sectional model vibration tests. In addition, they considered that the sectional model test would also eliminate the additional aerodynamic interference of the structural ancillary facilities. At the same time, compared with the full-bridge test, the taut strip model test has the characteristics of low cost and short duration, and can also consider the three-dimensional vibration of the structure. The taut strip model has been selected to replace the full-bridge aeroelastic model to perform the buffeting response test, and the results are compared with the prediction results based on the sectional model test in this paper. For this reason, the paper uses a long-span bridge with a basic section as an example, takes the turbulent characteristics simulated in the taut strip model test as the target wind

field, and relies on three different test techniques to predict the buffeting response of the structure. These techniques are as follows:

1. Identifying the aerodynamic parameters, such as aerodynamic admittance, through sectional model force measurement tests, and then calculating the response according to the traditional buffeting response calculation method;
2. Identifying the integrated transfer function of the structure through the sectional model vibration test, then predicting the buffeting response by using the method proposed by Su et al. [26];
3. Measuring the buffeting response of the structure through the taut strip model test.

Each buffeting response prediction result was then compared to investigate the long-span bridge buffeting response prediction methods based on the above three different test techniques and verify the accuracy and effectiveness of the prediction method based on the sectional model vibration test to identify the integrated transfer function.

## 2. Theoretical Analysis

At present, in the more commonly used analysis process, although the higher-order modes and the coupling effects between modes have a certain degree of influence on the structural buffeting response, the fundamental frequency still dominates [30]. Therefore, the coupling between modes in different directions is usually ignored without affecting the calculation accuracy. This paper will analyze the problem without considering the modal coupling effects. In addition, since the theoretical principles of the vertical, lateral and torsional buffeting responses are consistent, to simplify the derivation and demonstration process, this paper takes the vertical buffeting response as an example to study.

### 2.1. Traditional Buffeting Response Calculation

As mentioned above, most of the current bridge structure buffeting analysis uses Davenport's correction through the introduction of the aerodynamic admittance function into Scanlan's quasi-steady aerodynamic force expression. Although much work has been completed by many scholars to continuously improve the theories, these theoretical approaches are based on the pioneering work of Davenport and Scanlan.

Because the studies on buffeting by Su et al. [26] and Li et al. [27–29] used the wavenumber domain, in order to compare the traditional buffeting response calculation method with the following method, the buffeting response in the frequency domain is converted to the wavenumber domain for expression according to the relationship between the wavenumber and the frequency  $k = 2\pi n/U$ . Based on the random vibration theory and the buffeting analysis principle, the power spectrum of the bridge buffeting displacement response can be expressed as:

$$S_{h_i}(y, k_1) = \frac{\varphi_{h_i}^2(y)}{M_{h_i}^2} (2\rho U b C_L)^2 |\chi(k_1)|^2 |H_{h_i}(k_1)|^2 |J_{h_i}(k_1)|^2 S_u(k_1) \quad (1)$$

where  $S_{h_i}(y, k_1)$  is the power spectral density of the vertical buffeting displacement response at the axial coordinate  $y$  of the bridge;  $\varphi_{h_i}(y)$  is the  $i$ -th mode shape of the vertical motion;  $M_{h_i}$  is the vertical generalized mass;  $\rho$  is the air density;  $U$  is the mean wind velocity;  $b = B/2$  is the half-width of the bridge, where  $B$  is the width;  $C_L$  is the lift coefficient of the bridge section;  $k_1 = 2\pi n/U$  is the longitudinal wavenumber, where  $n$  is the frequency;  $\chi(k_1)$  is the one-wavenumber aerodynamic admittance function;  $H_{h_i}(k_1)$  is the vertical one-wavenumber frequency response function;  $J_{h_i}(k_1)$  is the vertical one-wavenumber joint acceptance function of the structure;  $S_u(k_1)$  is the longitudinal one-wavenumber fluctuating wind velocity spectrum.

As mentioned above, the traditional method for calculating the buffeting response is to identify the aerodynamic admittance and the aerodynamic derivative in the frequency response function of the bridge section through sectional model tests, and then obtain the power spectrum of the structural buffeting displacement response based on Equation (1).

Among them, the aerodynamic admittance function is an important transfer function for calculating the buffeting response, which is identified by the sectional model pressure or force measurement test. The RMS (root mean square) of the buffeting displacement can be obtained by integrating the buffeting response power spectrum:

$$\sigma_{h_i}^2(y) = \int_0^{+\infty} S_{h_i}(y, k_1) dk_1 \quad (2)$$

Finally, according to the SRSS (Square Root of Sum Square) method, the total buffeting response without considering the coupling effect between modes can be obtained:

$$\text{SRSS}(h_i) = \sqrt{\sigma_{h_{i,1}}^2 + \sigma_{h_{i,2}}^2 + \cdots + \sigma_{h_{i,m}}^2} \quad (3)$$

where  $m$  is the number of structural modes.

## 2.2. Calculation of Buffeting Response Based on Sectional Model Vibration Test

Traditional buffeting response calculation and analysis has always been based on the strip assumption; it divides the bridge into several strip units with independent aerodynamic properties in the spanwise direction, so as to obtain the aerodynamic response of the whole bridge through the integration along the spanwise direction [31]. From another perspective, it is assumed that the spanwise correlation of the buffeting force acting on the structure is equal to the correlation of the fluctuating wind. Based on the one-wavenumber aerodynamic admittance identified through methods such as wind tunnel tests to calculate the structural buffeting response, the calculation and analysis of the buffeting force and the buffeting response can be greatly simplified. However, many scholars [32–37] found that when the spanwise wavelength of the incoming flow is not much larger than the structure width, the three-dimensional effect of turbulence cannot be ignored, and the spanwise correlation of the buffeting force is much greater than that of the wind. This will lead to the failure of the strip assumption, which means that there will be a certain error in the calculation of the buffeting response of the bridge when using the traditional one-wavenumber aerodynamic admittance. This indicates that the influence of the spanwise wavenumber  $k_2$  should not be ignored when calculating the buffeting response of the structure. In turbulent analysis, compared with the autocorrelation of different turbulent fluctuation components, the influence of the cross-correlation is small and can be ignored [38–40]. To simplify the theoretical elaboration, according to the two-wavenumber buffeting analysis considering the three-dimensional effect of turbulence, and under the premise of ignoring the correlation between the horizontal fluctuating wind velocity and the vertical fluctuating wind velocity, the contribution of the longitudinal and vertical fluctuating wind velocities to the lift is equated to an equivalent aerodynamic admittance that considers the contribution of the fluctuating wind velocity in both directions to the lift. The two-wavenumber buffeting lift spectrum of a long-span bridge is:

$$S_{L_i}(k_1, k_2) = (\rho U b)^2 |\chi(k_1, k_2)|^2 \left[ 4C_L^2 |J_{u_{h_i}}(k_1, k_2)|^2 S_u(k_1) + (C_L' + C_D)^2 |J_{w_{h_i}}(k_1, k_2)|^2 S_w(k_1) \right] \quad (4)$$

where  $S_{L_i}(k_1, k_2)$  is the unsteady buffeting lift spectrum corresponding to the  $i$ -th mode of the structure;  $\chi(k_1, k_2)$  is the equivalent two-wavenumber aerodynamic admittance;  $C_D$  is the drag coefficient of the bridge section;  $C_L'$  represents the slope of the lift coefficient to the wind attack angle;  $J_{u_{h_i}}(k_1, k_2)$  and  $J_{w_{h_i}}(k_1, k_2)$  represent the two-wavenumber joint acceptance function corresponding to the longitudinal and vertical fluctuating wind velocities, respectively;  $S_w(k_1)$  is the vertical one-wavenumber fluctuating wind velocity spectrum.

According to recent theoretical and experimental studies [26–29] of the influence of the aspect ratio on the accuracy of the strip assumption and the three-dimensional effect of turbulence, for long-span bridges and other slender linear structures with large aspect ratios, the strip assumption is accurate enough. The influence of the spanwise wavenumber on the



aerodynamic admittance can be ignored in the calculation and analysis, and Equation (4) can be simplified as:

$$S_{L_i}(k_1, k_2) = (\rho U b)^2 |\chi(k_1)|^2 \left[ 4C_L^2 |J_{u_{h_i}}(k_1, k_2)|^2 S_u(k_1) + (C_L' + C_D)^2 |J_{w_{h_i}}(k_1, k_2)|^2 S_w(k_1) \right] \quad (5)$$

The one-wavenumber buffeting lift spectrum commonly used in the buffeting response calculation is easily obtained by integrating the above formula against  $k_2$ . At this time, it is consistent with the one-wavenumber buffeting lift spectrum in the process of the traditional calculation method in the previous section. The difference lies in the fact that the traditional buffeting analysis theory does not consider the influence of the three-dimensional effect of turbulence, which many scholars believe will cause a large error in the calculation of the buffeting response in the traditional buffeting analysis theory. The theoretical analysis mentioned earlier in this section pointed out that even if the influence of the turbulent three-dimensional effect is considered, as long as the turbulence integral scale is not much smaller than the structure width, the influence of the turbulent three-dimensional effect can also be ignored for long-span bridges and other linear slender structures with large aspect ratios [26–29]. The one-wavenumber aerodynamic admittance can be used instead of the two-wavenumber aerodynamic admittance, and the influence of the spanwise wavenumber  $k_2$  can be ignored. That is, the traditional buffeting analysis theory is considered to be accurate at this time. At present, the two-wavenumber buffeting analysis considering the three-dimensional effect of turbulence returns to the traditional buffeting theory analysis process, and the power spectral density function of the buffeting displacement response can also be expressed by Equation (1). In the formula, structural parameters such as geometric dimensioning, mode shape function, equivalent mass, natural frequency and damping ratio are only related to the inherent characteristics of the structure and do not change with the change of turbulence. The one-wavenumber aerodynamic admittance function only contains longitudinal wavenumbers, which reflects the aerodynamic transfer relationship between the 2D fluctuating velocity and the buffeting force, and can be expressed as a function of the dimensionless reduced frequency. It is only related to the bridge cross-section geometry and longitudinal wavenumber and has nothing to do with the characteristics of the turbulent flow field. In addition, considering the significance of buffeting research, and the fact that the study of the buffeting response is limited to ranges where the wind velocity is relatively small, the buffeting force is the main fluctuating load at this time, and the aerodynamic self-excited force accounts for a small proportion. Buffeting will not cause catastrophic consequences such as wind-induced flutter instability. It mainly affects comfort, safety and the fatigue damage of components in the use stage of the structure. Therefore, the study of buffeting under high wind velocity will, to some extent, be meaningless. For example, long-span bridges will be stopped when the wind velocity is high, limiting the passage of vehicles and pedestrians. Based on the above factors, Su et al. [26] proposed the concept of the integrated transfer function, which is the product of the one-wavenumber aerodynamic admittance and the one-wavenumber frequency response function. It is only determined by the structural characteristic parameters and has nothing to do with the turbulent flow characteristics:

$$|T_{h_i}(k_1)|^2 = |\chi(k_1)|^2 |H_{h_i}(k_1)|^2 \quad (6)$$

At this time, the buffeting response spectrum of the structure can be written as:

$$S_{h_i}(y, k_1) = \frac{\varphi_{h_i}^2(y)}{M_{h_i}^2} (2\rho U b C_L)^2 |T(k_1)|^2 |J_{h_i}(k_1)|^2 S_u(k_1) \quad (7)$$

Based on Equation (7), a sectional model with a reasonable aspect ratio can be selected for vibration testing to identify the integrated transfer function. Since the function has

nothing to do with the turbulent flow characteristics, it can be used to predict the buffeting response of bridge structures under any wind field by using Equations (1)–(3).

Two points need to be explained:

(1) Since the identification of the integrated transfer function is based on the measured value of the buffeting response at a certain point of the structure, when it is applied to the prediction of the buffeting response, the function identified at a point (such as the mid-span position of a long-span bridge) can only be used to predict the buffeting response of the actual structure at the same position;

(2) Due to the inconsistency between the mode shape functions of different orders, the integrated transfer functions corresponding to the mode shapes of different orders are also different. In other words, there is a fixed integrated transfer function corresponding to the different order mode shapes of the structure. Therefore, when using the integrated transfer function to predict the buffeting response of the actual structure, it is necessary to calculate the response of the different modes corresponding to the real bridge through the integrated transfer function of different orders, after which the SRSS method can be used to calculate the total response of the structure.

### 2.3. Buffeting Response Prediction Based on Taut Strip Model Test

The taut strip model buffeting response test is similar to the full-bridge aeroelastic model test. They both measure the 3D buffeting response of the 3D model under the action of 3D turbulence, but the former eliminates the additional aerodynamic interference of the structural ancillary facilities. The buffeting response spectrum  $S_h(y, k_1)$  of the structure under the simulated turbulent flow field is measured through the taut strip wind tunnel test, and the RMS of the buffeting response can then be calculated by Equation (8):

$$\sigma_h^2(y) = \int_0^{+\infty} S_h(y, k_1) dk_1 \quad (8)$$

## 3. Test Preparation

In the comparative study of different buffeting response calculation methods in this paper, taking a long-span bridge as the engineering background and taking the vertical buffeting response at the mid-span as an example, three test methods were used to predict and compare the buffeting response of the structure. It should be noted that considering the influence of the model aspect ratio on the three-dimensional effect [26–29], it is necessary to use a small scale ratio to make the model with a large aspect ratio in the sectional model test to minimize the influence of the three-dimensional effect of turbulence. This will lead to difficulty in the simulation of structures such as railings and maintenance channels in the sectional model test, so the 100% construction state of the bridge is selected as the research object.

### 3.1. Structural Overview

A long-span steel box girder suspension bridge was taken as an example to study in this paper. The main span of the bridge is 1020 m. The stiffening beam is an integral steel box girder with a width of 30.5 m and a height of 3.0 m. The tower height is 177.5 m, and the basic wind velocity is 25.0 m/s. The overall layout of the bridge structure is shown in Figure 1, and the standard cross-section of the main girder is shown in Figure 2.

### 3.2. Analysis of Structural Dynamic Characteristics

Structural dynamic characteristics constitute the premise of structural dynamic response analysis. Through the analysis of structural dynamic characteristics, the frequency distribution and mode shape characteristics of the structure can be understood, and parameters can be provided for the design of the wind tunnel test model. In this section, the ANSYS software is used to analyze and calculate the dynamic characteristics of the bridge.

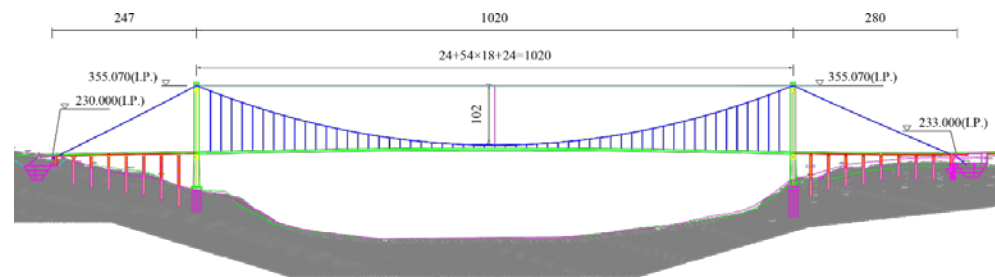


**Figure 1.** General layout drawing of the bridge (unit: m).

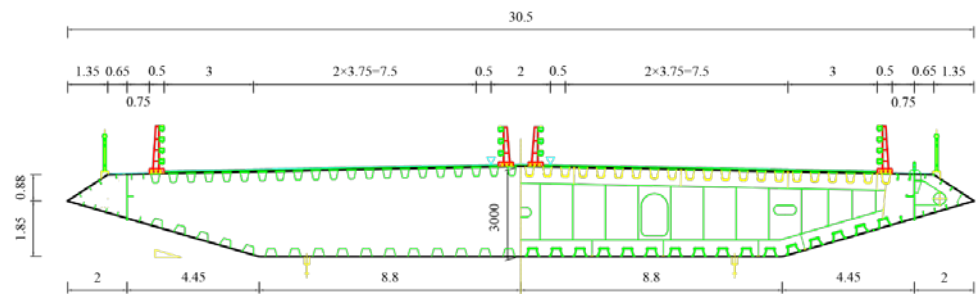


**Figure 2.** Standard cross-section of main beam (unit: m).

The calculation model of the bridge deck adopted the traditional “fishbone beam” model, as shown in Figure 3. The main girder and tower were discretized into three-dimensional beam elements (Beam4) according to the actual spatial position, the cables were discretized into three-dimensional cable elements (Link10), and the piers and junction piers were also discretized into three-dimensional beam elements (Beam4). The section properties and material properties of each element were assigned for the calculation. The mass and mass moment of inertia of the main beam were simulated by mass point element (Mass21).

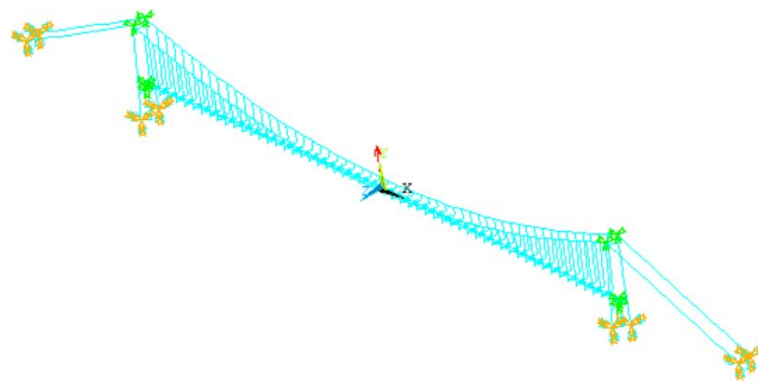


**Figure 3.** Bridge finite element model diagram.

The boundary constraints in the model were set as follows:

- (1) The bottom of the cable tower was embedded with the top surface of the cushion cap, that is, the degrees of freedom in six directions were restricted;
- (2) The main cable was fixed at the anchorage; the top connection of the main tower was a master–slave relationship;
- (3) The connection between the main beam and the main tower: The connection between the rotational degrees of freedom of the main beam in the transverse, vertical and around the bridge axis and the middle of the lower beam under the main tower was a master–slave relationship. The remaining three degrees of freedom were relaxed.



Using ANSYS software, the subspace iteration method was used to calculate the first 30-order frequencies and mode shapes of the bridge, which included three vertical modes:  $n_1 = 0.165$  Hz,  $n_2 = 0.230$  Hz and  $n_3 = 0.343$  Hz.

### 3.3. Test Equipment

The sectional model test was conducted in the XNJD-1 wind tunnel at Southwest Jiaotong University. The size of the test section was 16 m (length)  $\times$  2.4 m (width)  $\times$  2.0 m (height), and the wind velocity could be adjusted within a range of 1.0 to 45.0 m/s. In the vacant state of the wind tunnel, the turbulence intensity of the incoming flow was less than 0.5%, and the average airflow deflection angles in both the longitudinal and vertical directions were less than  $0.5^\circ$ . The taut strip model test was conducted in the XNJD-3 wind tunnel of Southwest Jiaotong University. The size of the test section was 36 m (length)  $\times$  22.5 m (width)  $\times$  4.5 m (height), and the wind velocity could be adjusted within a range of 1.0 to 16.0 m/s. The turbulence intensity of the incoming flow in the vacant state of the wind tunnel was less than 1%, and the average airflow deflection angles in both the longitudinal and vertical directions were less than  $1^\circ$ .

The turbulent wind field characteristics were collected using a TFI Cobra three-dimensional fluctuating anemometer (Cobra Probe), which is a four-hole pressure probe measuring instrument that can measure the real-time dynamic three-component velocity (longitudinal, horizontal and vertical), pitch angle and yaw angle. Its linear frequency measurement range is 0 Hz (uniform flow) to 2000 Hz, and its measurable wind velocity range is 2 m/s to 100 m/s. Its allowable error for measured wind velocity is  $\pm 0.1$  m/s, and its measurable wind direction angle range is  $\pm 45^\circ$ . The buffeting force measurement was conducted using a high-frequency dynamic six-axis force ATI Gamma balance, whose horizontal and vertical force ranges were 65 N and 200 N, respectively, with respective corresponding accuracies of 1/80 N and 1/40 N. The displacement response measurement used a non-contact laser displacement measurement sensor with a range of 200 mm and a static test accuracy of 40  $\mu\text{m}$ .

### 3.4. Turbulence Field Simulated

The taut strip model test was conducted in a large-scale wind tunnel, and passive simulation devices such as spires, baffles and rough elements were used to simulate the turbulent flow field, as shown in Figure 4.

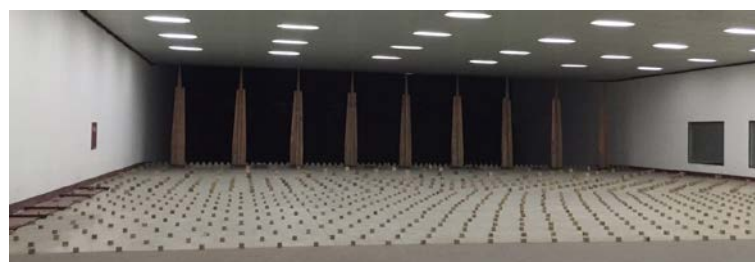


**Figure 4.** Spire turbulence field installed in XNJD-3 wind tunnel.

Because the turbulence integral scale simulated in the spire turbulence field is usually larger than that in the grid turbulence field, the test identification of the aerodynamic admittance and integrated transfer function of the structure were conducted in the simulated spire turbulence field, which can increase the ratio of the turbulence integral scale to the model width in order to minimize the influence of the turbulent three-dimensional effect. It can also simulate the shear layer characteristics, which is more convenient for analysis and comparison with the taut strip model test results. Therefore, the sectional model test was also conducted in a spire turbulence field, as shown in Figure 5.



**Figure 5.** Spire turbulence field installed in XNJD-1 wind tunnel.

To study the buffeting response under the turbulence field, it is necessary to first measure the flow field quality to ensure the accuracy of the study. It should be noted that, according to the buffeting theory of long-span bridges, it is not difficult to find that the fluctuating components of the turbulence field along the transverse wind direction do not contribute to the calculation of the buffeting response, so the transverse turbulent fluctuating characteristics were not repeated here. Among many turbulent fluctuating wind velocity spectrum models, the von Kármán spectrum [41], which is widely used in aviation and structural wind engineering, is more suitable for describing atmospheric turbulence higher above the ground and the turbulent characteristics simulated in a wind tunnel [42,43]. To ensure the quality of the simulated turbulence field in the test, it is usually fitted to the von Kármán spectrum. Figures 6 and 7 show the longitudinal and vertical fluctuating wind velocity spectrum of the above turbulence fields, and the von Kármán spectrum was used to fit the results. The results show that the simulated fluctuating wind velocity spectra fit well with the von Kármán spectrum, and met the test requirements.

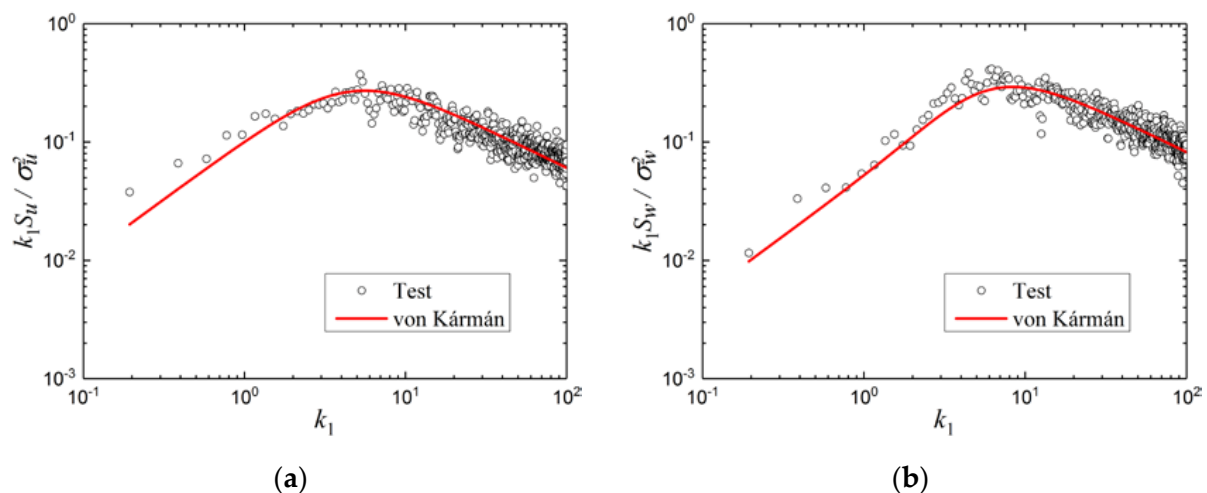


**Figure 6.** Longitudinal and vertical turbulence spectra in XNJD-1 spire turbulence field. (a) Longitudinal; (b) vertical.

In addition, Table 1 gives the other two important parameters of the turbulence field: turbulence intensity and turbulence integral scale. In Table 1,  $I$  and  $L$  represent the turbulence intensity and turbulence integral scale, respectively, and the subscripts  $u$  and  $w$  represent the longitudinal and vertical directions of the turbulence field, respectively.

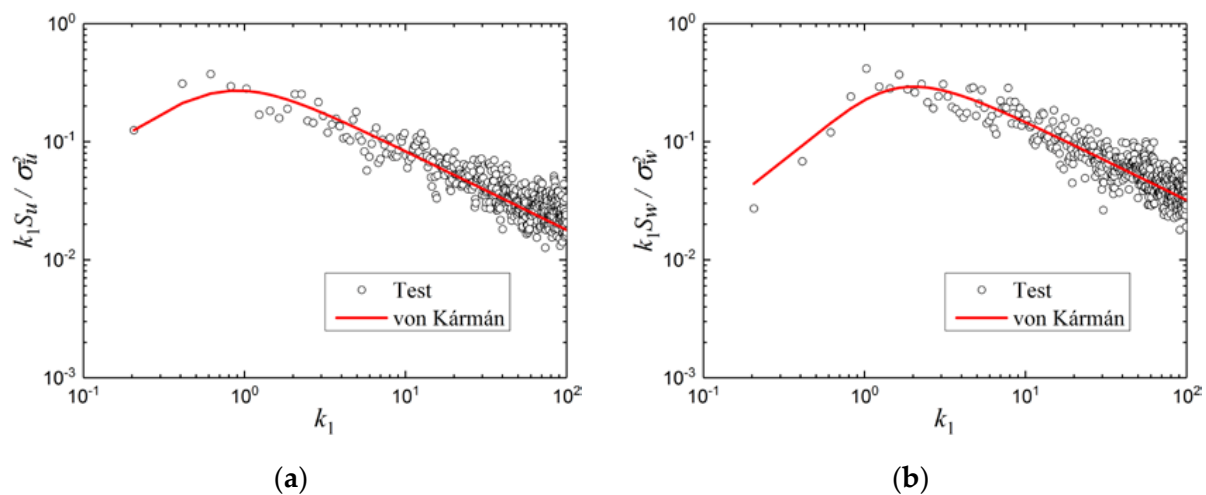


**Figure 7.** Longitudinal and vertical turbulence spectra in XNJD-3 spire turbulence field. (a) Longitudinal; (b) vertical.

**Table 1.** Turbulence characteristics parameters.

| Turbulence Field | Turbulence Intensity |       | Turbulence Integral Scale |       |
|------------------|----------------------|-------|---------------------------|-------|
|                  | $I_u$                | $I_w$ | $L_u$                     | $L_w$ |
| XNJD-1           | 14.2                 | 12.3  | 0.153                     | 0.092 |
| XNJD-3           | 15.7                 | 11.3  | 1.187                     | 0.650 |

#### 4. Test Arrangement

It should be noted that it is important to keep the dimensionless quantities consistent when using scaled models for wind tunnel testing. In the related tests in this paper, on the premise of ensuring that the bridge models were similar to the actual structure geometry, the sizes of the models that could effectively ensure the test operability were selected according to the sizes of the wind tunnels, and the geometric scale ratios were determined. Subsequently, based on the conversion relationship of geometric ratio, frequency ratio, and wind speed ratio, the model frequencies and test wind speeds were determined. The wind tunnel tests conducted at this time were considered to truly reflect the vibration performance of the bridge under the actual wind field.

##### 4.1. Three-Component Force Test

Through the static sectional model test of the stiffened beam, the three-component force coefficients were measured at different attack angles, and the results were provided for the subsequent prediction and analysis of the buffeting response of the structure. The sectional model of the stiffening beam, which was made of high-quality wood, adopted a geometric scale ratio of 1:50. The model was 2.095 m long, 0.61 m wide and 0.061 m high.

Stiffening beams were made of high-quality wood, and auxiliary facilities such as railings and maintenance tracks were carved from plastic plates as a whole according to the size of the drawings. The test was conducted in the XNJD-1 wind tunnel. The test section was equipped with a side wall support and a force balance system specially used for the static three-component force test of the bridge sectional model, and the attitude angle of the model (the angle of attack of the incoming flow relative to the model) was controlled by the computer. A three-component strain balance was used to measure the static three-component force. The sectional model ends were mounted directly on the three-component force test balance. In order to ensure the two-dimensional flow, end plates were set at both ends of the stiffening girder model to avoid the flow field being disturbed. The model installed in the wind tunnel is shown in Figure 8.



**Figure 8.** Three-component force test of sectional model.

#### 4.2. Aerodynamic Derivative Identification Test

The aerodynamic derivative identification test model was the same as the three-component force coefficient test model in the previous section. It was suspended on the bracket by eight tension springs to form a two-degree-of-freedom vibration system that could move vertically and rotate around the model axis. End plates were installed at both ends of the model to reduce the end effects and ensure the bidimensionality of the flow. The test support was placed outside the wind tunnel wall to avoid disturbing the turbulence field. The test model is shown in Figure 9.



**Figure 9.** Aerodynamic derivative identification test.

#### 4.3. Aerodynamic Admittance Identification Test

The traditional buffeting response calculation adopts the 2D one-wavenumber aerodynamic admittance combined with the correlation of the fluctuating wind. According to the research of Larose et al. on the influence of the three-dimensional effect, the commonly used aerodynamic admittance identified through sectional model tests is the generalized 3D one-wavenumber aerodynamic admittance. It is necessary to use the correlation of the buffeting force to calculate the buffeting response of long-span bridges. In recent years, based on studies by Su et al. [26] and Li et al. [27–29], it was found that, in addition to the ratio of the turbulence integral scale to the structure width, the aspect ratio is also an important parameter that controls the calculation accuracy of the buffeting response of long-span bridges. Even if the integral scale is close to or even slightly smaller than the structure width, as long as the structural aspect ratio is sufficient, the influence of the three-dimensional effect is very small, the strip assumption is valid, and the calculation of the buffeting response will also have high accuracy. At this time, the correlation of the fluctuating wind can be used instead of that of the buffeting force. Therefore, to minimize the influence of the three-dimensional effect, in the test identification of the aerodynamic admittance in this section and the integrated transfer function in the next section, under the premise that the test was conducted in the spire turbulence field with a large integral scale, a sectional model with a relatively large aspect ratio was used. The model was 1.35 m long and 0.15 m wide.

The identification of the 2D aerodynamic admittance was carried out in a spire-generated turbulent flow using the high-frequency force-balance measurement technique. The spires were 0.198 m and 0.160 m in width at the base and top, respectively, and 2.0 m in height. The distance between the spires was 0.8 m. The characteristics of turbulent wind field were measured using the TFI Cobra Probe. The three section models were supported on a steel platform approximately 4.5 m downstream of the spires, as shown in Figure 10. The test model was divided into three parts, namely the force model, two end plates ( $0.4 \text{ m} \times 0.3 \text{ m}$ ) and their connected pseudo-models (0.1 m in length). The gap between the pseudo-models and the force model was 1 mm. In addition, the balance and connections were covered by a fairing to prevent the influence of the incoming flow. The force measurement model was horizontally mounted at a 0-attack angle on the high-frequency dynamic balance.



**Figure 10.** Aerodynamic admittance function identification test.

#### 4.4. Integrated Transfer Function Identification Test

According to the structural scale ratio, the test wind velocity was taken as 2.2 m/s. Considering the influence of the scale ratio, simulating the high-order modes of the sectional model is very difficult. In this paper, only the first 30 modes of the 100% construction state of the structure were considered, including three vertical modes with respective frequencies of 0.165 Hz, 0.23 Hz and 0.343 Hz. The corresponding frequencies of the test model were 2.948 Hz, 4.01 Hz and 6.231 Hz, respectively. The model was 1.35 m long and 0.15 m wide. In the test, two laser displacement sensors were symmetrically arranged on both sides of the width direction of the model, and synchronous measurement was performed. The mean value of the buffeting response measured by the two sensors was the vertical buffeting response value of the structure. The integrated transfer function identification test is shown in Figure 11.



**Figure 11.** Integrated transfer function identification test.



#### 4.5. Taut Strip Model Test

Considering the size of the XNJD-3 wind tunnel and the span of the bridge, the scale ratio of the taut strip model was set to 1:100. The model was 10.2 m long and 0.305 m wide, and it was divided into 20 sections of equal length. Steel strands with a diameter of 2 mm were selected for the bracing wires, and the two ends of the steel strands connecting the models were anchored by screws to the end plates made of 10 mm thick steel. According to the similarity principle, the wind velocity ratio was 1:10 and the frequency ratio was 10:1. The test wind velocity was taken as 2.5 m/s. The three-order vertical frequencies of the model were 1.648 Hz, 2.304 Hz and 3.426 Hz, respectively. The taut strip model installed in the wind tunnel is shown in Figure 12.



Figure 12. Taut strip model test conducted in XNJD-3 wind tunnel.

### 5. Test Results

#### 5.1. Three-Component Force Coefficient

The static three-component force test was conducted in uniform flow. The test wind attack angles were  $\alpha = -12^\circ \sim +12^\circ$  and  $\Delta\alpha = 1^\circ$ . The static three-component force coefficient in the body-axis coordinate system is usually used for theoretical calculation and practical application. Figure 13 shows the relationship curve of the three-component force coefficient with the wind attack angle.

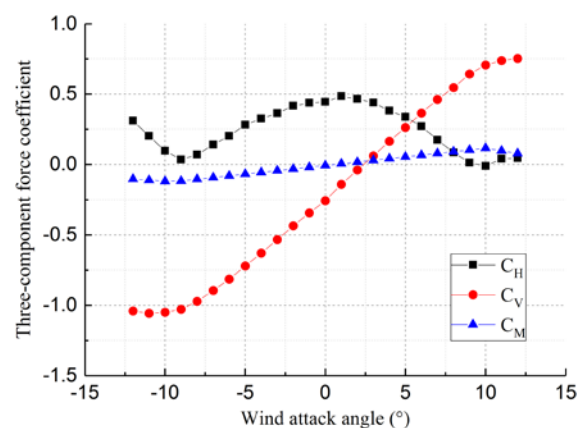
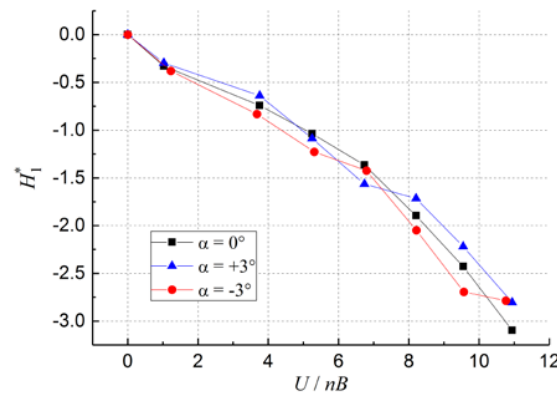


Figure 13. Three-component force coefficient curve of main beam in construction state.

#### 5.2. Aerodynamic Derivative

As mentioned above, the paper only takes the vertical buffeting response of the structure as an example, and it is only related to  $H_1^*$  in the aerodynamic derivatives. The result of  $H_1^*$  identified in the tests is shown in Figure 14.



**Figure 14.** Aerodynamic derivative  $H_1^*$  identification result.

### 5.3. Aerodynamic Admittance

The 2D aerodynamic admittance can be obtained through the 3D aerodynamic admittance identified by the test and the 3D effect influencing factor [44,45]:

$$\left| \chi_L^{2D}(k_1) \right|^2 = \frac{1}{g_L} \cdot \left| \chi_L^{3D}(k_1) \right|^2 \quad (9)$$

where  $\chi_L^{2D}(k_1)$  is the 2D one-wavenumber aerodynamic admittance;  $\chi_L^{3D}(k_1)$  is the 3D one-wavenumber aerodynamic admittance;  $g_L$  is the 3D effect influencing factor, and:

$$g_L = \frac{\int_{-\infty}^{+\infty} \sin^2(k_2 \delta) \left[ 4C_L^2 S_u(k_1, k_2) + (C_L' + C_D)^2 S_w(k_1, k_2) \right] dk_2}{\left[ 4C_L^2 S_u(k_1) + (C_L' + C_D)^2 S_w(k_1) \right]} \quad (10)$$

where  $\delta$  is the structural aspect ratio.

According to the above formulas, the 3D and 2D aerodynamic admittances of the structure were identified in the test, and the following general expression of the 2D aerodynamic admittance was used to fit the test results of the 2D aerodynamic admittance:

$$\left| \chi_L^{2D}(k_1) \right|^2 = \frac{1}{1 + \alpha k_1^\beta} \quad (11)$$

The two fitting parameters obtained were  $\alpha = 6.584$  and  $\beta = 1.444$ . In addition, the 3D aerodynamic admittance was inconsistent with the general expression of the above 2D aerodynamic admittance, so a fitting tool was used to fit it for application to the subsequent comparison of the buffeting response results. Figure 15 shows the identification results and fitting curves of the aerodynamic admittance.

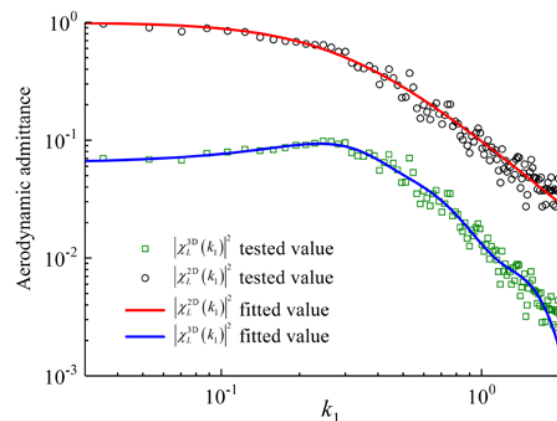


**Figure 15.** Aerodynamic admittance function identification result.

#### 5.4. Integrated Transfer Function

The measured buffeting response results of the three modes were combined, and the results are shown in Figure 16. V-S-1, V-S-2 and V-S-3 represent the first- to third-order vertical mode shapes of the structure, respectively.

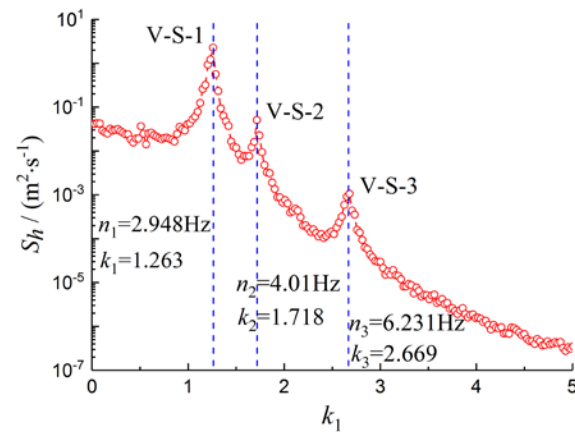


**Figure 16.** Vertical buffeting response of structure in XNJD-1 spire turbulence field.

As shown in the analysis results of the turbulence field characteristics simulated in the wind tunnel, the simulated turbulent fluctuating wind velocity spectrum conforms to the von Kármán spectral model. By substituting the turbulence field characteristic parameters into the von Kármán spectral model and combining them with the measured buffeting response of the structure, the integrated transfer function corresponding to each mode of the streamlined box girder can be calculated according to Equation (7). In addition, in order to clarify the displayed results, and based on the qualitative findings of Yang [45], Li [46], etc., who indicate that the results are less affected by the 3D effect at high-frequency positions while greatly affected at low-frequency positions, the test results of the integrated transfer function in this section are displayed in double logarithmic coordinates, as shown in Figure 17.

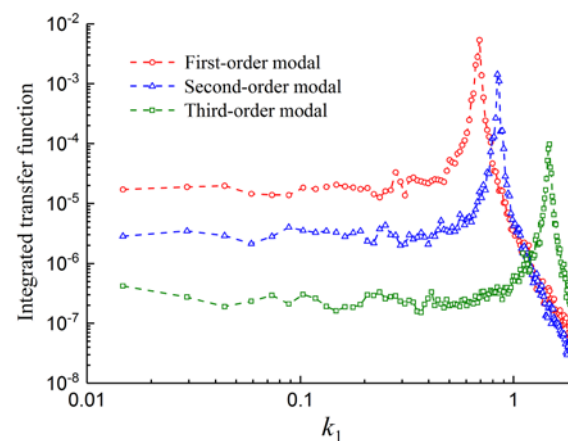


**Figure 17.** Integrated transfer function identification results.

#### 5.5. Taut Strip Model Test

In the taut strip model test, two laser displacement sensors were symmetrically arranged on both sides of the width direction of the model and synchronous measurement was performed. The mean value of the buffeting response measured by the two sensors was the vertical buffeting response value of the structure. The measured buffeting response results of the three modes were combined, and the results are shown in Figure 18.

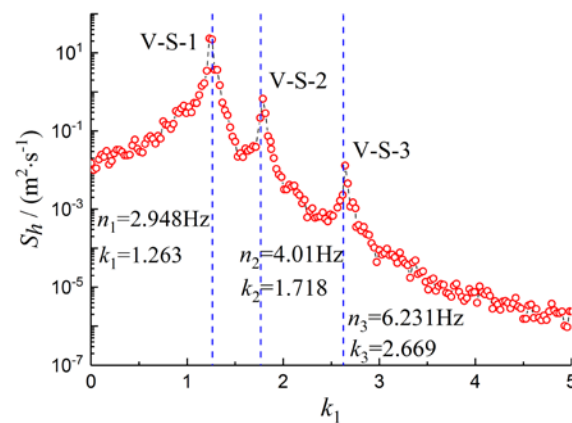


Figure 18. Buffeting response measured in taut strip model test.

## 6. Buffeting Response Prediction and Analysis

Relying on the aerodynamic admittance and aerodynamic derivative identified by the above sectional model test, the buffeting response result of the structure can be calculated according to Equations (1)–(3). Relying on the integrated transfer function identified by the sectional model vibration test, the prediction result of the buffeting response can be calculated according to Equation (7) and Equations (2) and (3). The buffeting response test result of the taut strip model can be calculated using Equation (8). A comparison of the three sets of results is shown in Figure 19. In addition, because the acquisition of the 2D aerodynamic admittance requires the identification of the 3D aerodynamic admittance, the results predicted using the 3D aerodynamic admittance and ignoring the influence of the aerodynamic admittance, based on the identification results of each aerodynamic admittance shown in Figure 12, are also displayed for comparison.

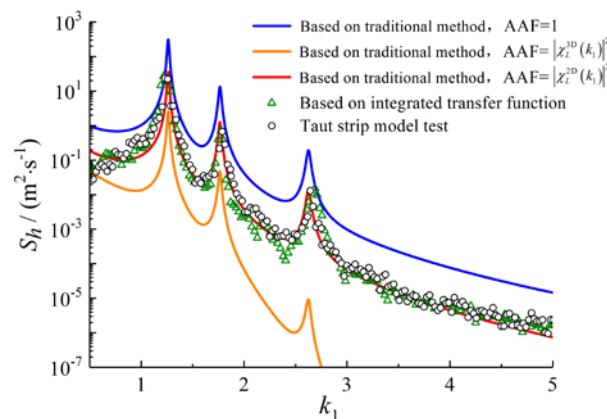


Figure 19. Buffeting response prediction results.

In Figure 18, the black and green scatter plots are the results of the taut strip model test and the prediction results based on the integrated transfer function, respectively. The solid curves with different colors are based on the traditional buffeting response calculation method, using the 2D and 3D aerodynamic admittances, respectively, and without considering the influence of the aerodynamic admittance. To facilitate this distinction and make the graph line clearer, the calculations based on the traditional method are based on the fitting formula of the aerodynamic admittance identification result.

As shown in the figure, there are three obvious main frequency peaks, which align well with the vertical natural frequency of the large-span bridge structure in the buffeting response prediction results obtained through different methods. The traditional buffeting response calculation method ignores the influence of the three-dimensional effect. Using the traditional sectional model test technique, which identifies the aerodynamic admittance

without considering the influence of the model aspect ratio, the traditional method uses the correlation of the fluctuating wind instead of the correlation of the buffeting force, which will cause a certain deviation in the calculation results. However, based on the research of Li et al. [27–29] regarding the influence of the aspect ratio on the accuracy of the strip assumption, it was found that when the integral scale is not much larger than the structure width, if the structural aspect ratio is sufficient, the three-dimensional effect can be ignored, and the strip assumption is accurate enough. At this time, the correlation of the fluctuating wind can be used to replace the correlation of the buffeting force; that is, the traditional buffeting response calculation method has high accuracy. Su et al. [26] then proposed the concept of the integrated transfer function and used it as the basis for a method for predicting the buffeting response of long-span bridges. The taut strip model test is carried out under the premise of accurately simulating the dynamic characteristics of the bridge. As shown in Figure 18, the buffeting response prediction results based on the identification of the 3D aerodynamic admittance and the integrated transfer function of the model with a large aspect ratio fit well with the taut strip model test results. We have reason to propose a reasonable sectional model test technique. That is, if the turbulence integral scale is not much larger than the structure width, the aspect ratio can be increased to make the traditional buffeting response calculation method and the method based on the integrated transfer function highly accurate. On the other hand, these two calculation methods are derived strictly based on Davenport's theory, so the two calculation results fit well with the theoretical expectations. In addition, this result also verifies from the side that Davenport and Scanlan's analysis methods based on the strip assumption apply to long-span bridges, and reveals the problems existing in the current identification methods for the aerodynamic parameters required in theory. A solution is also given, which is to select a reasonable aspect ratio to make the model.

On the other hand, the results show that the prediction results of the integrated transfer function identified based on the sectional model vibration test have high accuracy when using the effective test technique. This paper verifies the accuracy and applicability of the integrated transfer function proposed by Su et al. [26] in the buffeting response prediction of long-span bridges through effective tests for the first time. This paper rarely realizes the prediction of the buffeting response of long-span bridges through sectional model vibration tests, which broadens the application scope of sectional model tests to a certain extent, and improves the long-span bridge buffeting response prediction efficiency. It is more conducive to the consideration of the buffeting performance of the bridge during the aerodynamic selection in the preliminary design stage of the structure.

In addition, the calculation results using the 3D aerodynamic admittance are obviously small and become smaller and smaller as the wavenumber increases. This shows that when using the 3D aerodynamic admittance directly identified by the test, there is a large error in calculating the buffeting response using the correlation of the fluctuating wind. It is again demonstrated that when the influence of the three-dimensional effect is considered, the correlation of the fluctuating wind should not be used instead of the correlation of the buffeting force. The research of Larose et al. [32–37] on the three-dimensional effect is also verified from the opposite side. When the correlation of the fluctuating wind is used instead of the correlation of the force to calculate the buffeting response, a small buffeting response will be obtained, leading to an unsafe result.

However, ignoring the influence of the aerodynamic admittance, that is, in the case of  $AAF = 1$ , the buffeting response calculation result is higher. At this time, this means that the unsteady characteristics of the buffeting force are not considered, and the buffeting force acting on the main beam of the bridge can be calculated according to the quasi-steady theory. Obviously, for a bridge in the atmospheric boundary layer, the buffeting force acting on the bridge girder has strong unsteady characteristics, and ignoring the aerodynamic admittance will result in a more conservative analysis result.

It should be noted that this paper takes the streamlined box girder section as an example to compare various buffeting response prediction methods, and obtains the ex-



pected results. Although overall positive in terms of scientific significance, in view of the increasingly complex cross-section forms of current long-span bridges, the conclusions of this paper still need further in-depth research to verify applicability for other bridge cross-section forms.

## 7. Conclusions

Taking a long-span suspension bridge as an example, this paper predicts the buffeting response of the bridge under the design wind velocity in the simulated large-scale turbulence field through different calculation methods based on different sectional model test techniques. The research results show the following:

(1) The feasibility of the method for predicting the buffeting response of long-span bridges based on the integrated transfer function has been verified by an effective wind tunnel test for the first time. Through reasonable test methods, the integrated transfer function can be identified through the sectional model vibration test to predict the buffeting response of long-span bridges with high accuracy;

(2) The problems existing in the current test methods for identifying the theoretically required aerodynamic parameters are pointed out, and an effective solution is proposed. That is, if the turbulence integral scale is not much larger than the structure width, increasing the model's aspect ratio can effectively reduce the influence of the three-dimensional effect. This provides an effective technical means of predicting the buffeting response of long-span bridges in future sectional model tests;

(3) When the 3D aerodynamic admittance is used for the calculation of the buffeting response, if the correlation of the fluctuating wind is used instead of that of the buffeting force, a small buffeting response and an unsafe result will be obtained. Neglecting the effect of aerodynamic admittance will overestimate the buffeting response of long-span bridges and obtain a more conservative analysis result. The unsteady characteristics of the buffeting force should be considered when calculating the buffeting response of long-span bridges.

In conclusion, by adopting the reasonable test techniques (selecting a reasonable model aspect ratio for the test to reduce the influence of the 3D effect), the buffeting response prediction results obtained through the three kinds of wind tunnel tests aligned well with the expected results. Even so, there were still slight deviations in the results, which were mainly caused by reasons such as the coupling between modes being ignored in the sectional model vibration test, the influence of turbulence on self-excited forces and the motion state of structure being ignored in the rigid sectional model force test, the Reynolds number effect, etc. Considering that the wind tunnel test is still an indispensable method in the buffeting response prediction for bridges, more effective test techniques are required in subsequent research to further improve the accuracy of the prediction methods.

**Author Contributions:** Conceptualization, Y.S. and J.D.; methodology, Y.S. and J.D.; experiments, Y.S. and J.L.; validation, Y.S. and S.L.; investigation, Y.S., S.L. and B.J.; data curation, Y.S. and J.L.; writing—original draft, Y.S.; writing—review and editing, Y.S. and B.J.; supervision, J.D.; funding acquisition, J.D. All authors have read and agreed to the published version of the manuscript.

**Funding:** This work was financially supported by the National Key R&D Program of China (Grant No. 2021YFF0501004) and the National Natural Science Foundation of China (52008357).

**Institutional Review Board Statement:** Not applicable.

**Informed Consent Statement:** Not applicable.

**Data Availability Statement:** Data are contained within this article.

**Acknowledgments:** The authors thank the reviewers for their great help on the article during its review progress.

**Conflicts of Interest:** The authors declare no conflict of interest.

## References

1. Fung, Y.C. Fluctuating lift and drag acting on a cylinder in a flow at supercritical Reynolds numbers. *J. Aerosp. Sci.* **1960**, *27*, 801–814. [\[CrossRef\]](#)
2. Scruton, C. Aerodynamic buffeting on bridges. *Engineer* **1955**, *199*, 654–667.
3. Davenport, A.G. The response of slender, line-like structures to a gusty wind. *ICE Proc.* **1962**, *23*, 389–408. [\[CrossRef\]](#)
4. Davenport, A.G. Buffeting of a suspension bridge by storm winds. *J. Struct. Div.* **1962**, *88*, 233–270. [\[CrossRef\]](#)
5. Scanlan, R.H.; Tomko, J. Airfoil and bridge deck flutter derivatives. *J. Eng. Mech. Div.* **1971**, *97*, 1717–1737. [\[CrossRef\]](#)
6. Scanlan, R.H.; Gade, R.H. Motion of suspended bridge spans under gusty wind. *J. Struct. Div.* **1977**, *103*, 1867–1883. [\[CrossRef\]](#)
7. Scanlan, R.H. The action of flexible bridges under wind, I: Flutter theory. *J. Sound Vib.* **1978**, *60*, 187–199. [\[CrossRef\]](#)
8. Scanlan, R.H. The action of flexible bridges under wind, II: Buffeting theory. *J. Sound Vib.* **1978**, *60*, 201–211. [\[CrossRef\]](#)
9. Lin, Y.K.; Yang, J.N. Multimode bridge response to wind excitation. *J. Struct. Mech.* **1983**, *109*, 586–603. [\[CrossRef\]](#)
10. Kiviluoma, R. Coupled-mode buffeting and flutter analysis of bridges. *Comput. Struct.* **1999**, *70*, 219–228. [\[CrossRef\]](#)
11. Jain, A.; Jones, N.P.; Scanlan, R.H. Coupled flutter and buffeting analysis of long-span bridges. *J. Struct. Eng.* **1996**, *122*, 716–725. [\[CrossRef\]](#)
12. Xu, Z.; Wang, H.; Zhang, H.; Zhao, K.; Zhu, Q. Non-stationary turbulent wind field simulation of long-span bridges using the updated non-negative matrix factorization-based spectral representation method. *Appl. Sci.* **2019**, *9*, 5506. [\[CrossRef\]](#)
13. Kim, S.; Jung, H.; Kong, M.J.; Li, D.K.; An, Y.K. In-situ data-driven buffeting response analysis of a cable-stayed bridge. *Sensors* **2019**, *19*, 3048. [\[CrossRef\]](#)
14. Yan, L.; Ren, L.; He, X.; Lu, S.; Guo, H.; Wu, T. Strong wind characteristics and buffeting response of a cable-stayed bridge under construction. *Sensors* **2020**, *20*, 1228. [\[CrossRef\]](#)
15. Domaneschi, M.; Martinelli, L. Refined optimal passive control of buffeting-induced wind loading of a suspension bridge. *Wind Struct.* **2014**, *18*, 1–20. [\[CrossRef\]](#)
16. Chen, W.; Li, H.; Hu, H. An experimental study on the unsteady vortices and turbulent flow structures around twin-box-girder bridge deck models with different gap ratios. *J. Wind Eng. Ind. Aerodyn.* **2014**, *132*, 27–36. [\[CrossRef\]](#)
17. Li, H.; Chen, W.; Xu, F.; Li, F.; Ou, J. A numerical and experimental hybrid approach for the investigation of aerodynamic forces on stay cables suffering from rain-wind induced vibration. *J. Fluids Struct.* **2010**, *26*, 1195–1215. [\[CrossRef\]](#)
18. Chen, W.; Zhang, Q.; Li, H.; Hu, H. An experimental investigation on vortex induced vibration of a flexible inclined cable under a shear flow. *J. Fluids Struct.* **2015**, *54*, 297–311. [\[CrossRef\]](#)
19. Tao, T.; Wang, H.; Yao, C.; He, X. Parametric sensitivity analysis on the buffeting control of a long-span triple-tower suspension bridge with MTMD. *Appl. Sci.* **2017**, *7*, 395. [\[CrossRef\]](#)
20. Liu, H.; Lei, J.; Zhu, L. Identification and application of the aerodynamic admittance functions of a double-deck truss girder. *Appl. Sci.* **2019**, *9*, 1818. [\[CrossRef\]](#)
21. Gao, D.; Chen, W.; Li, H.; Hu, H. Flow around a circular cylinder with slit. *Exp. Therm. Fluid Sci.* **2017**, *82*, 287–301. [\[CrossRef\]](#)
22. Chen, W.; Gao, D.; Li, H.; Hu, H. Passive jet control of flow around a circular cylinder. *Exp. Fluids* **2015**, *56*, 201. [\[CrossRef\]](#)
23. Yan, L.; Zhu, L.; He, X.; Flay, R.G.J. Experimental determination of aerodynamic admittance functions of a bridge deck considering oscillation effect. *J. Wind Eng. Ind. Aerodyn.* **2019**, *190*, 83–97. [\[CrossRef\]](#)
24. Chen, W.; Xin, D.; Xu, F.; Li, H.; Ou, J.; Hu, H. Suppression of vortex-induced vibration of a circular cylinder using suction-based flow control. *J. Fluids Struct.* **2013**, *42*, 25–39. [\[CrossRef\]](#)
25. Laima, S.; Li, H.; Chen, W.; Li, F. Investigation and control of vortex-induced vibration of twin box girders. *J. Fluids Struct.* **2013**, *39*, 205–221. [\[CrossRef\]](#)
26. Su, Y.; Li, M. Integrated transfer function for buffeting response evaluation of long-span bridges. *J. Wind Eng. Ind. Aerodyn.* **2019**, *189*, 231–242. [\[CrossRef\]](#)
27. Li, M.; Yang, Y.; Li, M.; Liao, H. Direct measurement of the Sears function in turbulent flow. *J. Fluid Mech.* **2018**, *847*, 768–785. [\[CrossRef\]](#)
28. Li, M.; Li, M.; Yang, Y. A statistical approach to the identification of the two-dimensional aerodynamic admittance of streamlined bridge decks. *J. Fluids Struct.* **2018**, *83*, 372–385. [\[CrossRef\]](#)
29. Li, M.; Li, M.; Zhong, Y.; Luo, N. Buffeting response evaluation of long-span bridges with emphasis on three-dimensional effects of gusty winds. *J. Sound Vib.* **2019**, *439*, 156–172. [\[CrossRef\]](#)
30. Chen, X.; Kareem, A. Equivalent static wind loads for buffeting response of bridges. *J. Struct. Eng.* **2001**, *127*, 1467–1475. [\[CrossRef\]](#)
31. Fung, Y.C. *An Introduction to the Theory of Aeroelasticity*; John Wiley & Sons: New York, NY, USA, 1955.
32. Larose, G.L.; Livesey, F.M. Performance of streamlined bridge decks in relation to the aerodynamics of a flat plate. *J. Wind Eng. Ind. Aerodyn.* **1997**, *69*, 851–860. [\[CrossRef\]](#)
33. Larose, G.L.; Mann, J. Gust loading on streamlined bridge decks. *J. Fluids Struct.* **1998**, *12*, 511–536. [\[CrossRef\]](#)
34. Hjorth-Hansen, E.; Jakobsen, A.; Strømmen, E. Wind buffeting of a rectangular box girder bridge. *J. Wind Eng. Ind. Aerodyn.* **1992**, *42*, 1215–1226. [\[CrossRef\]](#)
35. Jakobsen, J.B. Span-wise structure of lift and overturning moment on a motionless bridge girder. *J. Wind Eng. Ind. Aerodyn.* **1997**, *69*, 795–805. [\[CrossRef\]](#)

36. Kimura, K.; Fujino, Y.; Nakato, S.; Tamura, H. Characteristics of buffeting forces on flat cylinders. *J. Wind Eng. Ind. Aerodyn.* **1997**, *69*, 365–374. [[CrossRef](#)]
37. Ma, C.; Wang, J.; Li, Q.; Liao, H. 3D aerodynamic admittances of streamlined box bridge decks. *Eng. Struct.* **2019**, *179*, 321–331. [[CrossRef](#)]
38. Ma, C. 3D Aerodynamic Admittance Research of Streamlined Box Bridge Decks. Ph.D. Thesis, Southwest Jiaotong University, Chengdu, China, 2007. (In Chinese)
39. Li, S.; Li, M.; Larose, G.L. Aerodynamic admittance of streamlined bridge decks. *J. Fluids Struct.* **2018**, *78*, 1–23. [[CrossRef](#)]
40. Su, Y.; Li, M.; Yang, Y.; Mann, J.; Liao, H.; Li, X. Experimental investigation of turbulent fluctuation characteristics observed at a moving point under crossflows. *J. Wind Eng. Ind. Aerodyn.* **2020**, *197*, 104079. [[CrossRef](#)]
41. von Kármán, T.; Howarth, L. On the statistical theory of isotropic turbulence. *Proc. R. Soc. Lond. Ser. A-Math. Phys. Sci.* **1938**, *164*, 192–215. [[CrossRef](#)]
42. Simiu, E.; Scanlan, R.H. *Wind Effects on Structures*; John Wiley & Sons: New York, NY, USA, 1996.
43. Xie, J.; Hunter, M.; Irwin, P. Experimental and analytical approaches in wind engineering studies for bridges. In Proceedings of the Budapest: Responding to Tomorrow's Challenges in Structural Engineering, Budapest, Hungary, 13–15 September 2006.
44. Li, M.; Li, M.; Su, Y. Experimental determination of the two-dimensional aerodynamic admittance of typical bridge decks. *J. Wind Eng. Ind. Aerodyn.* **2019**, *193*, 103975. [[CrossRef](#)]
45. Yang, Y. Aerodynamic Admittances of Airfoil and Rectangular Cylinder. Ph.D. Thesis, Southwest Jiaotong University, Chengdu, China, 2019. (In Chinese)
46. Li, M. Buffeting Response Analysis of Long-Span Bridges with Emphasis on the Three-dimensional Effects of Turbulence and the Study on the Equivalent Static Wind Loads. Ph.D. Thesis, Southwest Jiaotong University, Chengdu, China, 2019. (In Chinese)